Trends in continental temperature and humidity directly linked to ocean warming

Michael P. Byrne[a,b,1] and Paul A. O'Gorman[c]

[a]Space and Atmospheric Physics Group, Imperial College London, London SW7 2BW, United Kingdom; [b]Institute for Atmospheric and Climate Science, ETH Zürich, 8092 Zürich, Switzerland; and [c]Department of Earth, Atmospheric, and Planetary Sciences, Massachusetts Institute of Technology, Cambridge, MA 02139-4307

Edited by Isaac M. Held, Geophysical Fluid Dynamics Laboratory, National Oceanic and Atmospheric Administration, Princeton, NJ, and approved March 20, 2018 (received for review December 21, 2017)

In recent decades, the land surface has warmed substantially more than the ocean surface, and relative humidity has fallen over land. Amplified warming and declining relative humidity over land are also dominant features of future climate projections, with implications for climate-change impacts. An emerging body of research has shown how constraints from atmospheric dynamics and moisture budgets are important for projected future land–ocean contrasts, but these ideas have not been used to investigate temperature and humidity records over recent decades. Here we show how both the temperature and humidity changes observed over land between 1979 and 2016 are linked to warming over neighboring oceans. A simple analytical theory, based on atmospheric dynamics and moisture transport, predicts equal changes in moist static energy over land and ocean and equal fractional changes in specific humidity over land and ocean. The theory is shown to be consistent with the observed trends in land temperature and humidity given the warming over ocean. Amplified land warming is needed for the increase in moist static energy over drier land to match that over ocean, and land relative humidity decreases because land specific humidity is linked via moisture transport to the weaker warming over ocean. However, there is considerable variability about the best-fit trend in land relative humidity that requires further investigation and which may be related to factors such as changes in atmospheric circulations and land-surface properties.

continental climate change | temperature | humidity | atmospheric dynamics | moisture transport

Land–ocean contrasts are striking spatial fingerprints of global warming: Climate models predict that future changes in surface temperature will be strongly amplified over land (1–4) and that relative humidity will decline over land but remain approximately constant over oceans (5, 6). To predict and prepare for the impacts of climate change, it is critical to understand why continents and oceans respond so differently to global warming. Over recent years, simple constraints based on atmospheric dynamics and moisture transport have been introduced which link changes in surface-air climate over land and ocean regions and provide a physical explanation for land–ocean contrasts in model projections of future climate (3, 4, 6–10). These constraints imply that the land–ocean warming contrast occurs because air is drier over land than over ocean, and this causes a drop in land relative humidity which feeds back on the warming contrast. Note that the land–ocean warming contrast is not primarily due to the difference in thermal inertia between land and ocean, and it persists in equilibrium climate-change simulations (1, 3). However, it is not clear to what extent these constraints can be combined to explain the observed enhancement of warming over land in recent decades (1, 2, 11) or the strong decline in relative humidity over land since roughly 2000 (12, 13), especially given the complexity of land-surface processes.

Here we show using observations, the interim reanalysis (ERA-Interim) from the European Centre for Medium-Range Weather Forecasts and a simple analytical theory based on atmospheric dynamics and moisture transport that trends in continental temperature, specific humidity, and relative humidity can be estimated to first order using only changes in temperature over ocean and information about the climatological states over land and ocean.

Observed Trends

We first analyze surface-air temperature, specific humidity, and relative humidity changes over 1979–2016, averaged between 40°S and 40°N. Over land, we use the Met Office Hadley Centre's observational dataset HadISDH (13, 14). Over ocean, we use ERA-Interim reanalysis data (15) to overcome the sparsity of in situ surface-air observations, and we use climatological relative humidity to calculate specific humidity anomalies to avoid biases in the ERA-Interim specific humidity trends (see *Materials and Methods* for details). We focus on the 40°S to 40°N latitude band since the theory presented later is best justified at lower latitudes. Results for a tropical latitude band (20°S to 20°N) and a quasi-global latitude band (60°S to 80°N) are shown in *SI Appendix*, Figs. S1 and S2 and Table S1 and lead to similar conclusions.

The trends in continental and oceanic climates over 1979–2016 are shown in Fig. 1. Land temperatures have increased 42% more quickly than ocean temperatures (at a rate of 0.17 ± 0.04 K per decade vs. 0.12 ± 0.04 K per decade over oceans). All trends are calculated using ordinary least-squares regression and the uncertainty bounds represent the 90% confidence intervals of the best-fit trends corrected to account for serial correlation (16). By contrast, specific humidity has increased more quickly over oceans ($0.11 \pm 0.03\,\mathrm{g \cdot kg^{-1}}$ per decade) than over land

Significance

Changes in surface temperature and humidity over land are important for climate-change impacts on humans and ecosystems. Here, we show how trends in land humidity and temperature in recent decades are linked to ocean warming. While changes in temperature and humidity have been different over land and ocean, these changes have combined to give equal changes in the moist static energy of the air over land and ocean, consistent with expectations from atmospheric dynamics. We show how this dynamical constraint, and an additional constraint based on moisture transport, may be used to predict land climate changes given the ocean warming. Land surfaces are complex to understand and model, yet our results show a remarkably simple behavior of the climate system that emerges at large scales.

Author contributions: M.P.B. and P.A.O. designed research; M.P.B. performed research; M.P.B. analyzed data; and M.P.B. and P.A.O. wrote the paper.

The authors declare no conflict of interest.

This article is a PNAS Direct Submission.

[1]To whom correspondence should be addressed. Email: michael.byrne@imperial.ac.uk.

This article contains supporting information online at www.pnas.org/lookup/suppl/doi:10.1073/pnas.1722312115/-/DCSupplemental.

Published online April 23, 2018.

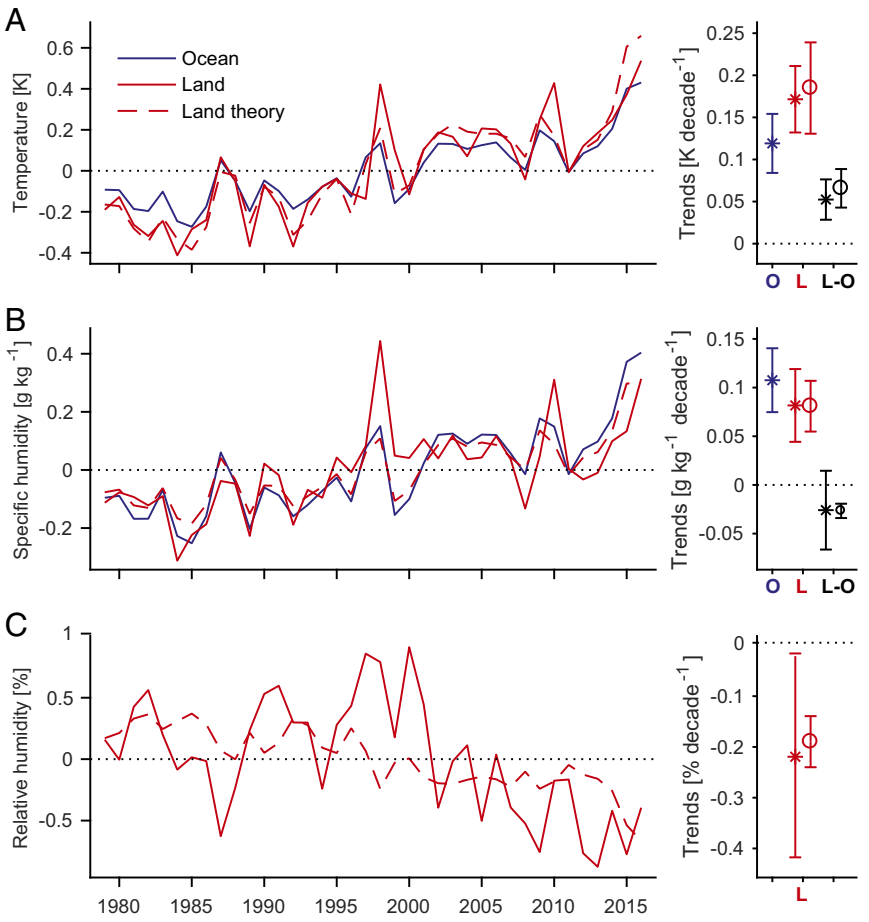

Fig. 1. (*A*–*C*) Surface-air annual (*A*) temperature, (*B*) specific humidity, and (*C*) relative humidity anomalies averaged from 40°S to 40°N and best-fit trends (1979–2016) over land (red solid lines and asterisks) and ocean (blue lines and asterisks). The best-fit trends in the land–ocean contrasts in temperature and specific humidity ($\delta T_L - \delta T_O$ and $\delta q_L - \delta q_O$, respectively) are also plotted (black asterisks). Land values are from the HadISDH dataset (13, 14) and ocean values are from the ERA-Interim reanalysis (15). Ocean specific humidity anomalies are calculated assuming fixed climatological relative humidity (*Materials and Methods*). Also shown are land anomalies and associated trends (dashed lines and circles) estimated using the simple theory (Eqs. **2**–**4**) and subsampled to the months and gridboxes for which HadISDH observations are available. Error bars on the trends indicate the 90% confidence intervals corrected to account for serial correlation (*Materials and Methods*).

($0.08 \pm 0.04\,\mathrm{g \cdot kg^{-1}}$ per decade), although the trend in the land–ocean difference is small compared with its uncertainty. There has been a decrease in relative humidity over continents but with large variability around the linear trend ($-0.22 \pm 0.20\%$ per decade, where % denotes the absolute rather than the fractional percentage change).

Ocean-Influence Theory

We now discuss a simple theory to help understand the amplified continental temperature and relative humidity responses to climate change. The theory combines two approximate physical constraints which link changes in surface-air temperatures and specific humidities over land and ocean. The atmospheric dynamics constraint (3, 4, 7, 9) is most easily justified at low latitudes where it follows as a consequence of weak horizontal temperature gradients in the free troposphere (17)—due to the effect of Earth's rotation being small at low latitudes—and active convection that maintains changes in surface moist static energy approximately equal to changes in saturated moist static energy aloft; this latter effect is known as convective quasi-equilibrium (18). As a result, changes in surface-air moist static energy at each latitude are equal over land and ocean (6),

$$\delta h_L = \delta h_O, \qquad [1]$$

where $h = c_p T + L_v q + g z_g$ is the surface-air moist static energy per unit mass of an air parcel, c_p is the specific heat capacity of air at constant pressure, T is absolute temperature, L_v is the latent heat of vaporization, q is the specific humidity, g is the gravitational acceleration, z_g is the geopotential height, the subscripts L and O denote land and ocean quantities, respectively, and here δ indicates an annual anomaly from the time mean over 1979–2016. Eq. **1** could also be phrased in terms of moist enthalpy because the surface geopotential term in the moist static energy remains constant (9) or in terms of other conserved variables such as the equivalent potential temperature (4, 7). The atmospheric dynamics constraint is found to be accurate for trends over recent decades, with similar trends in moist static energy averaged between 40°S and 40°N over land ($0.34 \pm 0.12\,\mathrm{kJ \cdot kg^{-1}}$ per decade) and ocean ($0.39 \pm 0.12\,\mathrm{kJ \cdot kg^{-1}}$ per decade) as shown in Fig. 2*A* (see *Materials and Methods* for details of the averaging used). This constraint also holds approximately between 20°S and 20°N (*SI Appendix*, Fig. S3*A*) and between 60°S and 80°N (*SI Appendix*, Fig. S4*A*).

The atmospheric moisture constraint (6, 10) relates changes in surface-air land and ocean specific humidities and predicts that fractional changes in specific humidity over land and ocean are equal. Two different approaches have been used to derive this atmospheric moisture constraint: One uses a control-volume

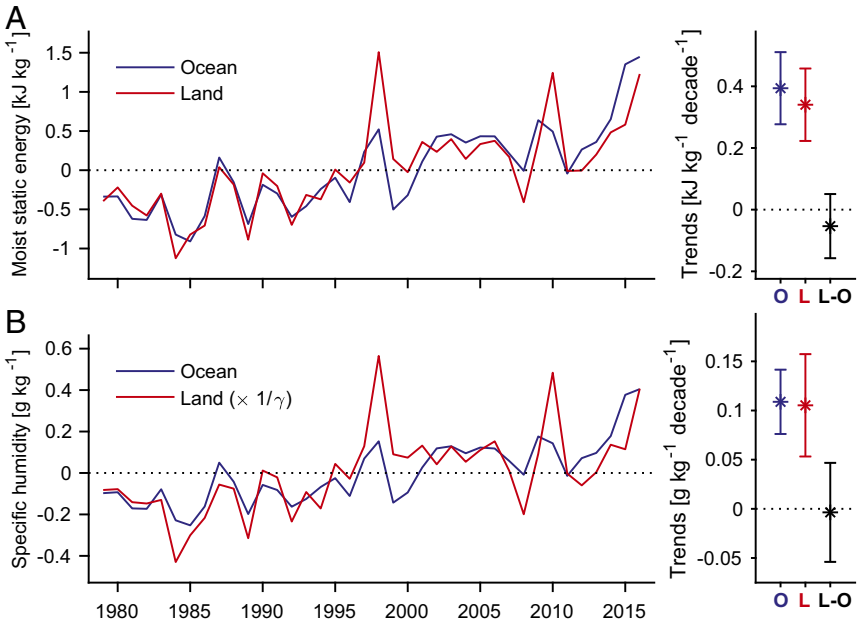

Fig. 2. (*A* and *B*) Surface-air annual (*A*) moist static energy and (*B*) specific humidity anomalies averaged from 40°S to 40°N and associated trends over oceans (blue lines and asterisks) and land (red lines and asterisks). The land specific humidity anomalies have been rescaled by a factor $1/\gamma$ so that equal trends over land and ocean correspond to the atmospheric moisture constraint holding (Eq. **2**). The best-fit trends in the land–ocean contrasts ($\delta h_L - \delta h_O$ and $\delta q_L/\gamma - \delta q_O$) are also shown (black asterisks). The land anomalies are calculated using observed temperatures and specific humidities from the HadISDH dataset, and the ocean anomalies are from the ERA-Interim reanalysis with climatological relative humidity (*Materials and Methods*). The parameter γ is the ratio of climatological land to ocean specific humidity from ERA Interim. The average of γ over land gridboxes between 40°S and 40°N is 0.72.

analysis of the boundary-layer moisture balance over land (6) and the other uses a Lagrangian analysis of air parcels (10). The moisture constraint predicts that changes in land specific humidity are a fraction, $\gamma = \overline{q_L}/\overline{q_O}$, of changes in neighboring ocean specific humidity, where $\overline{q_L}$ and $\overline{q_O}$ denote time averages over 1979–2016 of the land and ocean specific humidities, respectively. The moisture constraint is expressed as

$$\delta q_L = \gamma \delta q_O. \quad [2]$$

According to the boundary-layer moisture balance approach (6), the ratio γ in Eq. **2** is determined by horizontal and vertical mixing velocities in the atmosphere, heights of the boundary layers over land and ocean, and the vertical structure of specific humidity. We calculate γ for each land grid box using the zonal-mean ocean specific humidity at that latitude to represent the neighboring ocean following previous studies for climate-model projections (4, 6, 10). The ratio γ is approximately 0.7 in climate models (6) and is 0.72 in ERA-Interim data averaged between 40°S and 40°N. Consequently, changes in near-surface specific humidity over land are predicted to be approximately 70% of those over the ocean, and the atmospheric moisture constraint predicts a "land–ocean moistening contrast" with smaller increases in specific humidity over land than over ocean (but equal fractional changes over land and ocean). We find trends in specific humidity (40°S to 40°N) of $0.08 \pm 0.04\,\mathrm{g \cdot kg^{-1}}$ per decade over land and $0.11 \pm 0.03\,\mathrm{g \cdot kg^{-1}}$ per decade over ocean between 1979 and 2016 (Fig. 1*B*). The ratio of land to ocean trends is 0.76 which is roughly consistent with the prediction of 0.72 from the theory. Fig. 2*B* shows that the atmospheric moisture constraint also holds when the variation of γ across land grid boxes is taken into account. This constraint has also been tested in a variety of idealized and full-complexity climate models and is found to broadly capture simulated changes in land specific humidity under global warming (6, 10). Accurately estimating the changes in land relative humidity is more challenging, and the atmospheric moisture constraint substantially overestimates the decreases in relative humidity in northern midlatitudes in climate-model projections (6), possibly as a result of the large land fraction at these latitudes.

Combining the two constraints linking changes in temperatures and specific humidities over land and ocean, we can derive expressions for changes in continental temperature and relative humidity as a function of changes in the oceanic climate,

$$\delta T_L = \delta T_O + (1-\gamma)\frac{L_v}{c_p}\delta q_O \quad [3]$$

$$\frac{\delta r_L}{r_L} = \alpha(\gamma - 1)\frac{L_v}{c_p}\delta q_O, \quad [4]$$

where r_L is the surface-air relative humidity over land, $\alpha = L_v/R_v T^2 \approx 6\%/\mathrm{K}$ is the sensitivity of saturation vapor pressure to temperature (19), and R_v is the gas constant for water vapor. Eq. **3** follows directly from the dynamical and moisture constraints discussed above. In deriving Eq. **4** we have approximated relative humidity as the ratio of specific humidity to saturation specific humidity ($r = q/q^*$, where q^* is the saturation specific humidity) and used a linearized form of the Clausius–Clapeyron relationship to estimate fractional changes in saturation specific humidity ($\delta q^*/q^* = \alpha \delta T$). We have also assumed a constant ocean relative humidity because theory and models suggest only weak changes in ocean relative humidity (5, 19, 20). Available observations of ocean humidity are sparse but suggest that the assumption of small changes in ocean relative humidity is reasonable (*Materials and Methods*).

Eqs. **3** and **4** quantify the physical connection between changes in continental and oceanic climates, a connection which is mediated by dynamical and moisture constraints. Under global warming conditions, assuming that land surfaces are drier

than ocean surfaces in the current climate ($\gamma = \overline{q_L}/\overline{q_O} < 1$) and that specific humidity over oceans increases ($\delta q_O > 0$), Eqs. **3** and **4** predict that land will warm more than oceans ($\delta T_L > \delta T_O$) and that land relative humidity will decrease ($\delta r_L < 0$). According to this theory, the response of continental climate to increases in greenhouse gas concentrations is controlled by changes in ocean temperature and modulated by the present-day dryness of the land surface. Differences in land and ocean effective surface heat capacities are not needed to give a land–ocean warming contrast at a given latitude, but because the Southern Ocean warms slowly and has little neighboring land, the ratio of global-mean land warming to global-mean ocean warming can still be lower for equilibrium simulations compared with transient simulations as has previously been found (1, 3).

The physical theory for changes in land temperature and humidity, encapsulated in Eqs. **1**–**4**, approximately captures the observed long-term trends when subsampled to the HadISDH gridboxes and averaged from $40°$S to $40°$N (Fig. 1). The theory estimates for changes over land are evaluated at each land gridbox separately using zonal-mean ocean anomalies at that latitude. For temperature (Fig. 1*A*), the theory accurately predicts a warming trend of 0.18 ± 0.05 K per decade vs. an observed trend of 0.17 ± 0.04 K per decade. For specific humidity (Fig. 1*B*), the moisture constraint (Eq. **2**) predicts a moistening of $0.08 \pm 0.03\,\mathrm{g \cdot kg^{-1}}$ per decade vs. $0.08 \pm 0.04\,\mathrm{g \cdot kg^{-1}}$ per decade from observations. For relative humidity (Fig. 1*C*), the theory also captures the long-term land decrease ($-0.19 \pm 0.05\%$ per decade vs. $-0.22 \pm 0.20\%$ per decade in observations) although there is considerable variability about the trend that is not captured by the theory. The theory does similarly well for a tropical latitude band and a quasi-global latitude band (*SI Appendix*, Figs. S1 and S2 and Table S1). For the tropical latitude band, the warming contrast is weaker than for $40°$S to $40°$N because γ is higher in the deep tropics. The theory also gives similar results when observed sea-surface temperature (SST) anomalies from the Met Office Hadley Centre's dataset (HadSST3, refs. 21 and 22), rather than ERA-Interim surface-air temperature anomalies, are used over oceans to predict the changes in continental climate, although the land temperature trend estimate is less accurate (*SI Appendix*, Fig. S5).

Discussion

Remarkably, trends in continental temperature and humidity are broadly consistent with the simple dynamical and moisture constraints without explicit consideration of atmosphere or ocean circulation changes, cloud and aerosol radiative effects, soil moisture variability, land-use changes, or stomatal effects. Some of these additional factors, such as stomatal closure and changes in soil moisture, have been found to be important for climate-model projections of land relative humidity (9, 23), and to the extent that they alter γ they likely contribute to the large shorter-term variability in land relative humidity that is not captured by the theory, and they may also contribute to its longer-term trend which has a sizeable uncertainty compared with the trends in temperature and specific humidity (Fig. 1*C*). Here we are considering global-scale trends, and it is suggested that local land-surface changes have affected regional continental climate responses more strongly (24).

Even if changes in land-surface properties do not appear to be the dominant control of long-term trends over this period in global-scale continental temperature and humidity, the climatological land state (encoded in the γ parameter) is critical for partitioning a forced change in moist static energy into changes in temperature vs. specific humidity. Indeed in the simple theory it is because land surfaces are drier than ocean surfaces in today's climate ($\gamma < 1$) that continental temperature and relative humidity respond more strongly to global warming than oceanic temperature and relative humidity. The strong dependence of trends in continental climate on specific humidity in the current climate demonstrates the importance of simulating this property accurately in climate models to reliably predict future changes, and this is challenging given the complexity of the land surface (25).

Our results reveal that observed trends in continental climate over 1979–2016 are closely linked to neighboring ocean regions and can (to a first approximation) be estimated as a simple analytical function of the mean states of the land and ocean surfaces and the warming over ocean. Future work could apply extensions of the theory that explicitly consider circulation pathways and the effects of changes in soil moisture and stomatal behavior on boundary-layer moisture and the γ parameter to better understand the observed variability in land relative humidity. Given the utility of this simple quantitative framework in helping to explain the observed land–ocean contrasts in warming and moistening, it should also be a useful interpretive tool with which to interrogate proxy records of past continental climate change.

Materials and Methods

Temperature and Humidity Data over Land. Over land, surface-air (2-m) temperature, specific humidity, and relative humidity monthly anomalies are taken from the $5°$ latitude $\times$ $5°$ longitude HadISDH version 3.0.0.2016p dataset (13, 14). For all of the land time series calculated using HadISDH data, we use only the $5° \times 5°$ gridboxes that have at least 50% temporal coverage between 1979 and 2016. *SI Appendix*, Fig. S6 shows a map of the gridboxes with sufficient temporal coverage; there is good spatial coverage in midlatitudes, but it is relatively sparse in the tropics. Although HadISDH extends back to 1973, we choose 1979 as the start date for our analysis to be consistent with the ERA-Interim reanalysis (15), which is used for oceanic quantities and to evaluate γ in the simple theory.

ERA-Interim Reanalysis Data. We use the ERA-Interim reanalysis ($1.5° \times 1.5°$, 2-m data) to provide full spatial coverage over oceans. We also use it for climatological specific humidity over land when evaluating γ in the simple theory because the climatological values from HadISDH have less spatial coverage than the anomalies. Monthly surface-air specific and relative humidity data are not freely available for ERA Interim, and therefore we estimate the 2-m specific humidity for each month between 1979 and 2016 and for each gridbox using 6-hourly ERA-Interim dewpoint temperatures and surface pressures. We calculate the 6-hourly specific humidity from the 2-m dewpoint temperature and the surface pressure using the moist thermodynamics formulation outlined by Simmons et al. (1999) (26) and then average over each month between 1979 and 2016. To estimate the monthly 2-m relative humidity, we first calculate the saturation and actual vapor pressures using 6-hourly surface pressures and 2-m temperatures and dewpoint temperatures at each gridbox, before taking the ratio of these vapor pressures and averaging over each month between 1979 and 2016. Because of a change in the underlying SST data assimilated by the reanalysis (27), we uniformly increase the ERA-Interim surface-air ocean temperatures by 0.1 K from 2002 onward. Furthermore, following Simmons et al. (12), for ocean regions we use 6-hourly output data from the ERA-Interim 6-h background forecast to avoid issues related to uncorrected biases in air-temperature observations from ships (28) (for land regions the analysis data are used). Despite this approach, there remain biases in the ocean humidity trends that are discussed in detail below, and so we set the relative humidity over ocean to the climatological values, consistent with expectations of small changes in relative humidity over ocean. Specifically, we assume a constant ocean relative humidity for each calendar month and gridbox (averaged from 1979 to 2001 to avoid the aforementioned issue with ERA-Interim ocean surface-air temperatures after 2001) and use the relationship between temperature, specific humidity, and relative humidity to calculate the ocean specific humidity anomalies required for Eqs. **1**–**4**. This approach results in ocean specific humidity anomalies and trends that are generally consistent with 10-m surface-air specific humidity observations from the National Oceanographic Center Surface Flux and Meteorological Dataset (NOCS, version 2.0) (29) when subsampled to the observations (*SI Appendix*, Fig. S7*D* and Table S2) and ocean surface-air temperature anomalies that behave similarly to SST anomalies from observations (*SI Appendix*, Fig. S7*B* and Table S2).

Averaging in Space and Time. We first calculate anomalies with respect to 1979–2016 means. We then spatially average the gridboxes (only those with sufficient temporal coverage over land) with cosine-latitude weighting over the specified region, before computing annual-average values. These average anomalies are used for all figures and trends except for Fig. 2 and *SI Appendix*, Figs. S3 and S4. For the moist static energy and specific humidity anomalies in Fig. 2 and *SI Appendix*, Figs. S3 and S4, we first average zonally, then average meridionally with cosine-latitude weighting, and then calculate annual-average values. This approach (with zonal and then meridional averages) is the consistent way with which to evaluate the dynamics and moisture constraints when neighboring ocean is taken to be the zonal mean over ocean, and it avoids biases that would otherwise arise due to variations in land fraction (and data coverage) with latitude.

Estimation of Trends and Uncertainties. Trends over 1979–2016 for each time series are calculated using ordinary least-squares regression with uncertainty bounds representing the 90% confidence intervals of the best-fit trends corrected to account for serial correlation using an effective sample size (16). The 90% confidence intervals in Figs. 1 and 2 suggest the trends in Fig. 1 are significant at the 0.1 level for δT_L, δT_O, $\delta T_L - \delta T_O$, δq_L, δq_O, and δr_L but not for $\delta q_L - \delta q_O$. For Fig. 2, the land trends and ocean trends are significant at this level, but the land–ocean difference trends are not (as would be expected if the constraints hold). Using the 0.05 level would give the same results but with the observed δr_L trend in Fig. 1 insignificant. However, an important caveat for these results is that adjusting a confidence interval for a known serial correlation using an effective sample size can make the interval too wide, whereas errors in estimating the effective sample size make rejection of a null hypothesis more likely (30).

Application of the Simple Theory to Estimate Continental Climate Change. We evaluate the simple theory for continental temperature and relative humidity anomalies (Eqs. **3** and **4**), and the moisture constraint to predict land specific humidity anomalies (Eq. **2**), for all land regions for which gridded surface-air observations (HadISDH) are available. Land temperature, specific humidity, and relative humidity anomalies for each month and gridbox on the ERA-Interim grid are estimated using the specified equations, before being linearly interpolated to the HadISDH grid and subsampled at the months and gridboxes for which land observations are available (taking into account the specified 50% threshold for temporal coverage, as discussed above). Land anomalies relative to climatological monthly values for 1979–2016 are estimated for each month and gridbox before taking spatial and annual averages—these average anomalies are used for the theory results in Figs. 1 and 2 and *SI Appendix*, Figs. S1–S5 and Table S1.

The ocean temperature and specific humidity anomalies on the right-hand sides of Eqs. **2**–**4** are zonal averages over all ERA-Interim ocean gridboxes at the latitude of the land temperature or humidity anomaly being estimated. Similarly, the parameter γ is calculated using ERA-Interim data for each land gridbox by taking the average specific humidity at that point for the given calendar month over 1979–2016 and dividing by the specific humidity for that calendar month averaged over 1979–2016 and zonally over all ocean gridboxes at the same latitude as the land gridbox.

Need for Use of Reanalysis Data over Ocean and Comparison with Observations. Reanalysis data over ocean are needed because using surface-air observational data as an input to the theory is problematic because of insufficient spatial coverage. For example, 10-m surface-air temperature from NOCS (29) has reliable data for only 46% of the ocean when averaged from 40°S to 40°N and over 1979–2014 (the annual-average coverage has also declined by 31% between 1979 and 2014). By comparison, HadISDH has coverage for 71% of land between 40°S and 40°N averaged from 1979–2016 (*SI Appendix*, Fig. S6), and this coverage is relatively stable over time. A new marine version (no. 1.0.0.2016p) of the HadISDH dataset is in test phase (31, 32) and has greater mean spatial coverage (54%) that is more constant over time (less than 15% decrease in coverage between 1979 and 2016) compared with NOCS, but it was found to give noisy results when used as an input to the simple theory, presumably because of the very sparse coverage at some latitudes.

We compare observed temperature and humidity anomalies over land and ocean to ERA-Interim data in *SI Appendix*, Fig. S7 and Table S2. For this comparison, we interpolate and subsample the ERA-Interim data to HadISDH over land, to the SST dataset HadSST3 for ocean temperatures, to NOCS for ocean specific humidities, and to a test version of the marine HadISDH dataset for ocean relative humidities. In each case, we first interpolate the ERA-Interim data to the observational grid and then subsample at the gridboxes and months for which observational data are available (only observational gridboxes with greater than 50% temporal coverage are used for plotting the time series and calculating trends).

Anomalies from ERA Interim are similar to the observed HadISDH anomalies for temperature, specific humidity, and relative humidity over land (*SI Appendix*, Fig. S7 *A*, *C*, and *E*) although there are some discrepancies in the magnitudes of the trends (*SI Appendix*, Table S2). ERA-Interim surface-air ocean temperature anomalies are comparable to observed SST anomalies from HadSST3 (*SI Appendix*, Fig. S7*B*), which supports the use of ERA Interim for ocean temperature anomalies since the air-surface temperature difference is not expected to change greatly over ocean.

However, the trends in ERA-Interim specific and relative humidity contrast substantially with available observations over oceans (*SI Appendix*, Fig. S7 *D* and *F* and Table S2). For ocean specific humidity, ERA Interim shows a substantially weaker upward trend compared with NOCS. For ocean relative humidity, ERA Interim shows a large decreasing trend ($-0.40 \pm 0.09\%$ per decade) for the 40°S to 40°N latitude band, but the test version of the marine HadISDH dataset (31, 32) has approximately constant relative humidity ($-0.02 \pm 0.14\%$ per decade). (NOCS does not report relative humidity values, but if we estimate them from the NOCS monthly temperature and specific humidity values we find an increasing ocean relative humidity trend that seems to be related to a different temperature trend than found in the other datasets.) Theory and modeling suggest that surface-air ocean relative humidity should not change greatly as climate warms (5, 19, 20), and the discrepancies between ERA-Interim ocean humidity trends and observations where available cast doubt on the fidelity of the ERA-Interim trends in ocean humidity, and therefore we use climatological ocean relative humidities as discussed above.

ACKNOWLEDGMENTS. We are grateful to the Met Office Hadley Center for providing the HadISDH (https://www.metoffice.gov.uk/hadobs/hadisdh/) and HadSST3 (https://www.metoffice.gov.uk/hadobs/hadsst3/) datasets, to the National Oceanographic Center for providing the NOCS Surface Flux and Meteorological Dataset (noc.ac.uk/science/sustained-observations/noc-surface-flux-dataset/), and to the European Center for Medium-Range Weather Forecasts for providing the ERA-Interim reanalysis (https://www.ecmwf.int/en/forecasts/datasets/reanalysis-datasets/era-interim). M.P.B. acknowledges support from the Imperial College London Research Fellowship Scheme, and P.A.O. acknowledges support from NSF Grant AGS-1552195.

1. Sutton RT, Dong B, Gregory JM (2007) Land/sea warming ratio in response to climate change: IPCC AR4 model results and comparison with observations. *Geophys Res Lett* 34:L02701.
2. Lambert FH, Chiang JCH (2007) Control of land-ocean temperature contrast by ocean heat uptake. *Geophys Res Lett* 34:L13704.
3. Joshi MM, Gregory JM, Webb MJ, Sexton DMH, Johns TC (2008) Mechanisms for the land/sea warming contrast exhibited by simulations of climate change. *Clim Dyn* 30:455–465.
4. Byrne MP, O'Gorman PA (2013) Link between land-ocean warming contrast and surface relative humidities in simulations with coupled climate models. *Geophys Res Lett* 40:5223–5227.
5. O'Gorman PA, Muller CJ (2010) How closely do changes in surface and column water vapor follow Clausius-Clapeyron scaling in climate-change simulations? *Environ Res Lett* 5:025207.
6. Byrne MP, O'Gorman PA (2016) Understanding decreases in land relative humidity with global warming: Conceptual model and GCM simulations. *J Clim* 29:9045–9061.
7. Byrne MP, O'Gorman PA (2013) Land-ocean warming contrast over a wide range of climates: Convective quasi-equilibrium theory and idealized simulations. *J Clim* 26:4000–4016.
8. Sherwood SC, Fu Q (2014) A drier future? *Science* 343:737–739.
9. Berg AM, et al. (2016) Land-atmosphere feedbacks amplify aridity increase over land under global warming. *Nat Clim Change* 6:869–874.
10. Chadwick R, Good P, Willett KM (2016) A simple moisture advection model of specific humidity change over land in response to SST warming. *J Clim* 29:7613–7632.
11. Karl TR, et al. (2015) Possible artifacts of data biases in the recent global surface warming hiatus. *Science* 348:1469–1472.
12. Simmons AJ, Willett KM, Jones PD, Thorne PW, Dee DP (2010) Low-frequency variations in surface atmospheric humidity, temperature, and precipitation: Inferences from reanalyses and monthly gridded observational data sets. *J Geophys Res* 115:D01110.
13. Willett KM, et al. (2014) HadISDH land surface multi-variable humidity and temperature record for climate monitoring. *Clim Past* 10:1983–2006.

14. Smith A, Lott N, Vose R (2011) The integrated surface database: Recent developments and partnerships. *Bull Am Meteorol Soc* 92:704–708.
15. Dee DP, et al. (2011) The ERA-Interim reanalysis: Configuration and performance of the data assimilation system. *Quart J R Meteorol Soc* 137:553–597.
16. Santer BD, et al. (2000) Statistical significance of trends and trend differences in layer-average atmospheric temperature time series. *J Geophys Res Atmos* 105:7337–7356.
17. Sobel AH, Bretherton CS (2000) Modeling tropical precipitation in a single column. *J Clim* 13:4378–4392.
18. Emanuel KA (2007) Quasi-equilibrium dynamics of the tropical atmosphere. *The Global Circulation of the Atmosphere*, eds Schneider T, Sobel AH (Princeton Univ Press, Princeton), pp 186–218.
19. Held IM, Soden BJ (2006) Robust responses of the hydrological cycle to global warming. *J Clim* 19:5686–5699
20. Schneider T, O'Gorman PA, Levine XJ (2010) Water vapor and the dynamics of climate changes. *Rev Geophys* 48:RG3001.
21. Kennedy JJ, Rayner NA, Smith RO, Parker DE, Saunby M (2011) Reassessing biases and other uncertainties in sea surface temperature observations measured in situ since 1850: 1. Measurement and sampling uncertainties. *J Geophys Res Atmos* 116:D14103.
22. Kennedy JJ, Rayner NA, Smith RO, Parker DE, Saunby M (2011) Reassessing biases and other uncertainties in sea surface temperature observations measured in situ since 1850: 2. Biases and homogenization. *J Geophys Res Atmos* 116:D14104.
23. Cao L, Bala G, Caldeira K, Nemani R, Ban-Weiss G (2010) Importance of carbon dioxide physiological forcing to future climate change. *Proc Natl Acad Sci USA* 107:9513–9518.
24. Findell KL, Shevliakova E, Milly PCD, Stouffer RJ (2007) Modeled impact of anthropogenic land cover change on climate. *J Clim* 20:3621–3634.
25. Seneviratne SI, et al. (2010) Investigating soil moisture-climate interactions in a changing climate: A review. *Earth Sci Rev* 99:125–161.
26. Simmons AJ, Untch A, Jakob C, Kållberg P, Unden P (1999) Stratospheric water vapour and tropical tropopause temperatures in ECMWF analyses and multi-year simulations. *Quart J R Meteorol Soc* 125:353–386.
27. Simmons AJ, Poli P (2015) Arctic warming in ERA-Interim and other analyses. *Quart J R Meteorol Soc* 141:1147–1162.
28. Simmons AJ, et al. (2004) Comparison of trends and low-frequency variability in CRU, ERA-40, and NCEP/NCAR analyses of surface air temperature. *J Geophys Res Atmos* 109:D24115.
29. Berry DI, Kent EC (2011) Air–sea fluxes from ICOADS: The construction of a new gridded dataset with uncertainty estimates. *Int J Climatol* 31:987–1001.
30. Zwiers FW, von Storch H (1995) Taking serial correlation into account in tests of the mean. *J Clim* 8:336–351.
31. Willett KM (2017) HadISDH-marine.1.0.0.2016p – gridded global surface humidity dataset. Available at https://www.metoffice.gov.uk/hadobs/hadisdh/indexMARINE.html. Accessed September 8, 2017.
32. Freeman E, et al. (2017) ICOADS release 3.0: A major update to the historical marine climate record. *Int J Climatol* 37:2211–2232.